

Real-Time Interactive Hybrid Ocean: Spectrum-Consistent Wave Particle-FFT Coupling

Shengze Xue^(✉), Yu Ren, Jiacheng Hong, Run Ni, Shuangjiu Xiao^(✉), and Deli Dong^(✉)

Digital ART Lab, Shanghai Jiao Tong University, Shanghai, China
{richardxue,xiaosj,arli@sjtu.edu.cn}
<http://dalab.se.sjtu.edu.cn/www/home/>

Abstract. Fast Fourier Transform-based (FFT) spectral oceans are widely adopted for their efficiency and large-scale realism, but they assume global stationarity and spatial homogeneity, making it difficult to represent non-uniform seas and near-field interactions (e.g., ships and floaters). In contrast, wave particles capture local wakes and ripples, yet are costly to maintain at scale and hard to match global spectral statistics.

We present a real-time interactive hybrid ocean: a global FFT background coupled with local wave-particle (WP) patch regions around interactive objects, jointly driven under a unified set of spectral parameters and dispersion. At patch boundaries, particles are injected according to the same directional spectrum as the FFT, aligning the local frequency-direction distribution with the background and matching energy density, without disturbing the far field.

Our approach introduces two main innovations: (1) Hybrid ocean representation. We couple a global FFT background with local WP patches under a unified spectrum, achieving large-scale spectral consistency while supporting localized wakes and ripples. (2) Frequency-bucketed implementation. We design a particle sampling and GPU-parallel synthesis scheme based on frequency buckets, which preserves spectral energy consistency and sustains real-time interactive performance. Together, these innovations enable a unified framework that delivers both large-scale spectral realism and fine-grained interactivity in real time.

Keywords: computer animation · ocean simulation · sea wave spectrum · real-time simulation · wave particle · fast fourier transform.

1 Introduction

In virtual reality, visual effects, maritime training, and digital twin applications, realistic, dynamic, and interactive ocean-surface simulation is essential. Real oceans exhibit strong spatiotemporal variability and non-uniformity—shaped by wind seas, swell, depth, and other factors[20]—and include localized disturbances such as ship wakes and floater ripples. These macro-micro features jointly challenge visual immersion and physical plausibility.

State-of-the-art large-scale ocean synthesis commonly adopts spectral, FFT-based methods[4,14], which superpose directional-spectrum waves in the frequency domain to generate periodic surfaces, achieving efficient, globally consistent results for film and games. However, like Gerstner-wave stacking[6], FFT methods assume spatial homogeneity and global stationarity, offering limited local control and struggling to reproduce ship wakes, floater ripples, shallow-water effects, and other localized phenomena with precision. By contrast, the Wave Particle approach introduced by Yuksel[23] and refined by Jeschke et al.[10,11] targets real-time water interaction rather than large-area synthesis: it propagates wave particles with physical attributes to flexibly generate locally non-uniform disturbances from moving objects, excelling at high-fidelity near-field detail. Yet maintaining vast particle counts at scale is costly, and the resulting local field is difficult to keep consistent with the global ocean in energy distribution and spectral statistics. More complex particle-only methods such as PBF[13] and SPH[17] are even more expensive and typically limited to small-scale offline rendering.

This situation yields an “impossible triangle” in large-scale ocean simulation: statistical models like FFT scale efficiently[21]; wave-based particle methods enable local interaction and non-uniformity; but simultaneously achieving real-time performance, global consistency, and fine near-field interaction remains unresolved.

To address this, we propose a real-time interactive hybrid ocean. An FFT ocean serves as the global background wave field, while wave particle patch regions are introduced around interactive objects. The two representations share unified spectral parameters and dispersion; particles are injected at patch boundaries according to the same spectrum as the background, ensuring local spectral and energy distributions match the global field. With frequency bucketing and parallel reconstruction, the wave particle energy field is efficiently composed into height maps and smoothly fused with the global FFT ocean, yielding seamless transitions between near and far fields. Our method resolves this “impossible triangle” by combining the efficiency of FFT with the interactivity of WP under a consistent spectrum. Specifically, our contributions are:

Hybrid ocean representation. A novel WP–FFT coupling under a unified spectrum that integrates large-scale stability with localized interactions.

Frequency-bucketed implementation. A new wave particle sampling and GPU-parallel synthesis scheme that maintains spectral consistency while enabling real-time performance.

2 Previous Work

Wave simulation methods and ocean modeling methods both reproduce water-surface dynamics but differ in focus. Wave simulation centers on generating wave fields via spectral, particle, or fluid formulations with prescribed statistics or dynamics, largely independent of scene geometry and boundary conditions,

emphasizing plausibility and efficiency. Ocean modeling emphasizes integrated behavior under specific boundaries, coupling global and local representations across resolutions so that one domain shows far-field state and near-field interaction.

2.1 Wave Simulation Methods

FFT-based spectral methods superpose directional-spectrum components in the frequency domain and invert to height fields, yielding efficient, large-scale, globally consistent oceans[4,14]. They leverage spectra such as Phillips[18] and JONSWAP[15], are GPU-friendly, and power systems like Crest[2], but assume spatial homogeneity and global stationarity, limiting local control and fidelity for wakes, ripples, and shallow-water effects. wave particle methods[10,11,23] target real-time interaction, generating locally non-uniform disturbances from moving objects, yet become costly at scale and struggle to stay consistent with global spectral statistics. Pan et al.[19] combine spectral control with wave particles for local control, but remain fundamentally particle-based and thus insufficient for real-time, very large domains.

2.2 Ocean Modeling Methods

Huang[9] couples high-resolution FLIP[1] in the near field with a far-field BEM[12], exchanging boundary data bidirectionally. The framework delivers physically consistent transitions and convincing visuals but inherits the high cost of 3D particle fluids, limiting real-time scalability to large oceans.

In summary, spectral methods are efficient but lack local control; wave particle methods enable interaction but do not scale; and full 3D fluid couplings are too expensive for real time. We therefore propose a real-time interactive hybrid ocean that fuses a global FFT background with local wave particle regions under unified spectral parameters, preserving large-scale frequency characteristics while achieving detailed, physically continuous interactions.

3 Method

This paper presents a real-time interactive hybrid ocean that couples a globally spectral, FFT-driven ocean with local Lagrangian wave particle patch regions. In this model, the primary wave field is synthesized via Fast Fourier Transform to ensure spectral consistency and computational efficiency at large scales, while detailed disturbance zones near interactive objects (e.g., ships, floaters) are reconstructed with wave particles to realize local non-uniformity and interactivity. To guarantee a seamless transition and physical consistency between the two representations, all wave particles are initialized from the same spectral parameters as the FFT and are generated under a statistical energy-density constraint, so that their energy expression and visual appearance remain compatible with the background wave field.

3.1 Hybrid Ocean Representation

The proposed hybrid ocean comprises two complementary wave representations: (i) a global background wave field synthesized by a spectral FFT, producing a large-scale, continuous, spectrum-consistent surface; and (ii) local wave particle patch regions placed around interactive objects to reconstruct non-uniform, disturbance-responsive near-field waves. The two are coupled at the parameter level by sharing a unified directional spectrum and dispersion relation.

The FFT ocean takes a directional spectrum as input and composes periodic waves in the frequency domain, well suited to statistically steady far-field behavior. Because computation is concentrated in the frequency domain and the entire height map is updated by a single inverse transform, local control is difficult. In contrast, wave particles provide a Lagrangian description of propagation: each particle carries direction, frequency, and amplitude, and contributes locally via a kernel. This makes the particle model adaptable to localized disturbances, particularly in highly interactive zones such as wakes and crest interference.

To fuse the two consistently in space, we adopt a local replacement strategy: around each interactive object, a rectangular wave particle patch region is defined, the FFT representation is disabled inside, and the surface is provided by the wave particle field. At patch boundaries, particles are injected according to the same directional spectrum as the FFT background, yielding a smooth transition in energy distribution, directional structure, and visual appearance. To avoid double counting or depletion of energy, the patch contribution is composited only locally; the global height field is obtained by stitching the background with all patch regions.

In this project we adopt the JONSWAP spectrum as the global spectral model and use a multiplicative directional spreading:

$$S_J(\omega, \theta) = S_J(\omega) Dir(\omega, \theta) \quad (1)$$

where ω is the angular frequency, θ is the angle between wave and wind directions, $S_J(\omega)$ gives the frequency-domain energy distribution, and $Dir(\omega, \theta)$ is the directional spreading function.

Compared with the Phillips spectrum, JONSWAP is defined over the joint frequency-direction domain[3], better fitting measured ocean energy distributions and, via the peak-enhancement factor γ , capturing wind-sea growth over finite fetch and duration[8]. Its one-dimensional form is:

$$S_J(\omega) = \alpha g^2 \omega^{-5} \exp \left[-\frac{5}{4} \left(\frac{\omega_p}{\omega} \right)^4 \right] \gamma^r \quad (2)$$

with

$$r = \exp \left[-\frac{(\omega - \omega_p)^2}{2\sigma^2 \omega_p^2} \right] \quad (3)$$

where ω_p is the peak frequency, σ controls the peak width, and γ is the peak-enhancement factor. We use the standard parameterizations:

$$\alpha = 0.076 \left(\frac{U_{10}^2}{Fg} \right)^{0.22}, \quad \omega_p = 22 \left(\frac{g^2}{U_{10}F} \right)^{1/3}, \quad \gamma = 7.0 \left(\frac{gF}{U_{10}^2} \right)^{-0.142} \quad (4)$$

where U_{10} is the wind speed at 10 m height, F is the fetch, and g is gravitational acceleration.

We employ the commonly used *cos-2s* spreading, and the function should be normalized[5]:

$$\text{Dir}(\omega, \theta) = \frac{\Gamma(s(\omega) + 1)}{2\sqrt{\pi} \Gamma(s(\omega) + \frac{1}{2})} \left[\cos\left(\frac{\theta}{2}\right) \right]^{2s(\omega)}, \quad \int_{-\pi}^{\pi} \text{Dir}(\omega, \theta) d\theta = 1 \quad (5)$$

In the above, $\Gamma(\cdot)$ is the Gamma function used for normalization, and s is the spreading parameter that controls directional concentration around the mean wave direction. Following the observations of Mitsuyasu et al.[16], we parameterize $s(\omega)$ as

$$s(\omega) = 16.0 \left(\frac{\omega}{\omega_p} \right)^{\mu}, \quad \mu = \begin{cases} 5.0, & \omega \leq \omega_p, \\ -2.5, & \omega > \omega_p, \end{cases} \quad (6)$$

This hybrid representation directly enables the coexistence of large-scale consistency and fine-grained local detail, as highlighted in our contributions.

With the spectral update of the FFT background field being a well-established procedure, the remainder of this method focuses on how to generate and drive wave particle patch regions under the same spectrum.

3.2 Spectrum-Based Initialization of Single wave particle

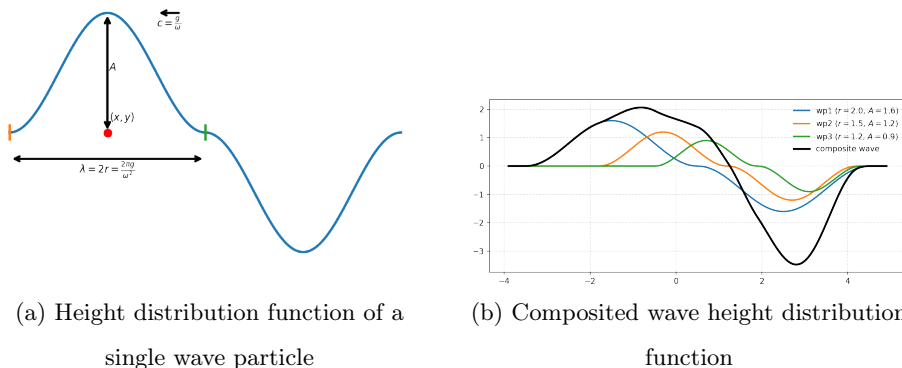


Fig. 1. Wave height functions of a single wave particle (including the positive-negative pair) and of a wave composed of multiple particles.

In the hybrid ocean model, the wave particle patch region must inherit consistent statistical characteristics from the spectrum to ensure continuity with the global FFT background in both energy structure and visual appearance. An

intuitive illustration of how wave particles superpose into waves is shown in 1. To this end, we adopt the spectrum-guided initialization proposed by Pan et al.[19], sampling each wave particle’s attributes from a unified directional spectrum, including angular frequency ω , propagation direction θ , wavelength λ , amplitude A , and dispersion parameter k . This sampling process is aligned with the directional spectrum used by the FFT background, enabling spectrum-driven coherent evolution.

Particles are sampled over (ω, θ) . In deep water ($\omega^2 = gk$, $k = 2\pi/\lambda$) [18], for fixed ω :

$$k = \frac{\omega^2}{g}, \quad \lambda = \frac{2\pi}{k} = \frac{2\pi g}{\omega^2} \Rightarrow r = \frac{\lambda}{2} = \frac{\pi g}{\omega^2}, \quad c = \frac{\omega}{k} = \frac{g}{\omega}.$$

The particle amplitude A can be computed from the spectral energy density function $S(\omega, \theta)$ [3]:

$$A = \sqrt{2S(\omega, \theta)\Delta\omega\Delta\theta} \quad (7)$$

Thus once ω and θ are given, A , r , and c are uniquely determined, ensuring spectral energy consistency.

Within the hybrid ocean simulation framework, however, maintaining energy continuity between the local wave particle patch region and the global FFT background requires continuous particle injection at the patch boundaries. The key challenge lies in estimating an appropriate distribution of particle counts across frequencies ω and directions θ under given wind and directional spectrum conditions—particularly balancing the abundance of high-frequency short waves against the scarcity of low-frequency long waves.

3.3 Spectrum-Based Estimation of wave particle Distribution

The JONSWAP spectrum function $S(\omega, \theta)$ describes the distribution of ocean surface wave energy in the frequency-direction domain under given wind speed and wind direction. By integrating this spectrum over the entire frequency-direction plane, the total energy density per unit surface area can be obtained:

$$\bar{E} = \int_{\omega_{\min}}^{\omega_{\max}} \int_{-\pi}^{\pi} S(\omega, \theta) d\theta d\omega \quad (8)$$

In implementation, we define the sampling frequency range as $[0.5\omega_p, 2.5\omega_p]$ to ensure efficiency and avoid noise[22]. Instead of using a uniform step size, we divide it into N_ω frequency buckets by equal-energy partitioning. The sampling strategy is shown in Figure 2. The total energy density of a frequency bucket containing all waves with frequency ω_i can then be expressed as:

$$\bar{E}_{\omega_i} = \int_{-\pi}^{\pi} S(\omega_i, \theta) d\theta \cdot \Delta\omega_i \quad (9)$$

Here, $\Delta\omega_i$ is the bucket width, i.e., the sampling interval. Since all waves in the bucket share the same frequency ω_i , their phase speed is uniquely determined as

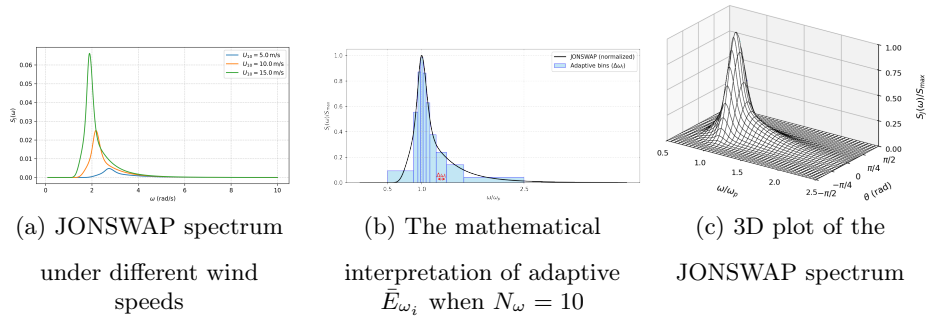


Fig. 2. Representation of the JONSWAP Spectrum and Sampling Strategy

$c_i = \frac{g}{\omega_i}$. Over a boundary of length L , during a time step Δt , the area swept by waves of frequency ω_i is:

$$\Delta S_{\omega_i} = L \cdot \Delta t \cdot c_i = L \cdot \Delta t \cdot \frac{g}{\omega_i} \quad (10)$$

For simplicity, let the patch region be a square. When considering only net inflow energy, the sum over the four sides cannot be written as $4\Delta S$, since some waves propagate outward. However, inflow and outflow on opposite sides cancel out. Thus, for a square of side length L , the total swept area of incoming waves can be expressed as:

$$\Delta S_{\omega_i, \text{square}} = 2 \cdot \Delta S_{\omega_i} = 2L \cdot \Delta t \cdot \frac{g}{\omega_i} \quad (11)$$

Thus, over a time step Δt , the total incoming energy of waves with frequency ω_i into the region is:

$$\begin{aligned} \mathcal{E}_{\omega_i, \text{square}} &= \rho g \cdot \Delta S_{\omega_i, \text{square}} \cdot \bar{E}_{\omega_i} \\ &= 2\rho g L \cdot \Delta t \cdot \frac{g}{\omega_i} \cdot \int_{-\pi}^{\pi} S(\omega_i, \theta) d\theta \cdot \Delta\omega_i \end{aligned} \quad (12)$$

On the other hand, from the wave particle perspective, the energy of a single deep-water wave particle with frequency ω_i and direction θ_j is:

$$\begin{aligned} \mathcal{E}_{\omega_i, \theta_j} &= \frac{1}{8} \rho g A_{\omega_i, \theta_j}^2 \pi r_i^2 \\ &= \frac{1}{8} \rho g \cdot 2S(\omega_i, \theta_j) \Delta\omega_i \Delta\theta \cdot \pi \left(\frac{\pi g}{\omega_i^2} \right)^2 \\ &= \frac{1}{4} \rho g \Delta\omega_i \frac{\pi^3 g^2}{\omega_i^4} S(\omega_i, \theta_j) \Delta\theta \end{aligned} \quad (13)$$

Wave particles sharing the same frequency ω_i but spanning all directions θ_j are referred to as a group. The total energy of 1 group at frequency ω_i is:

$$\mathcal{E}_{\omega_i, group} = \frac{1}{4} \rho g \Delta\omega_i \frac{\pi^3 g^2}{\omega_i^4} \sum_{j=1}^{N_\theta} S(\omega_i, \theta_j) \Delta\theta \quad (14)$$

If within a time step Δt , the number of particle groups of frequency ω_i entering the square region is N_i , then:

$$\begin{aligned} \mathcal{E}_{\omega_i, square} &= N_i \cdot \mathcal{E}_{\omega_i, group} \\ &= N_i \cdot \frac{1}{4} \rho g \Delta\omega_i \frac{\pi^3 g^2}{\omega_i^4} \sum_{j=1}^{N_\theta} S(\omega_i, \theta_j) \Delta\theta \end{aligned} \quad (15)$$

When N_θ is sufficiently large, the summation in (15) can be approximated to:

$$\sum_{j=1}^{N_\theta} S(\omega_i, \theta_j) \Delta\theta \approx \int_{-\pi}^{\pi} S(\omega_i, \theta) d\theta \quad (16)$$

By comparing equations(12) and(15), the number of particle groups with frequency ω_i entering the square region within a time step Δt is:

$$N_i = \frac{8L \cdot \Delta t \cdot \omega_i^3}{\pi^3 g} \quad (17)$$

Specifically, if the region is a rectangle with side lengths L_1 and L_2 , then the number of particle groups N_i generated on opposite sides should correspond to two values:

$$N_{i_1} = \frac{4L_1 \cdot \Delta t \cdot \omega_i^3}{\pi^3 g}, \quad N_{i_2} = \frac{4L_2 \cdot \Delta t \cdot \omega_i^3}{\pi^3 g} \quad (18)$$

Thus, we obtain the number of particles to be generated in each frequency bucket per time step under the energy consistency constraint.

It is worth noting that Eq.(17,18) have clear physical meaning: its units reduce to a dimensionless particle group count, matching the derivation goal. The result is intuitive—particle groups scale with Δt and L , and grow rapidly with frequency ω_i , reflecting the abundance of short waves versus the rarity of long waves in real seas. Although N_ω and N_θ are decoupled from particle counts, this is reasonable: increasing N_θ raises particle numbers but lowers individual amplitudes, preserving energy. Thus the injection rule is both mathematically consistent and physically sound.

4 Implementation

4.1 Pipeline Overview

Each frame update follows the pipeline shown in Fig 3. At a high level, both the global FFT field and local WP patches are updated under the same spectrum, then combined into the final hybrid ocean.

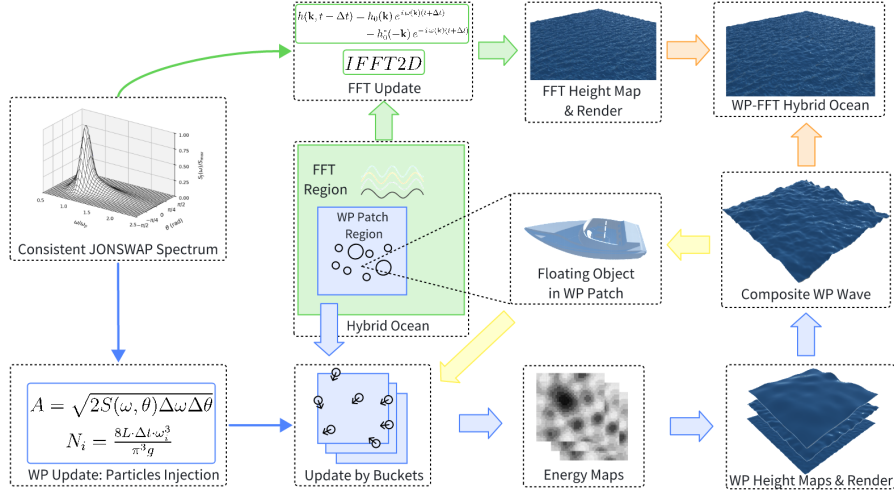


Fig. 3. Pipeline overview. Green arrows indicate FFT updates, blue arrows indicate wave particle (WP) updates, orange arrows indicate coupling between FFT and WP, and yellow arrows indicate interactions between floating objects and WP patches. Both branches are driven by the same spectrum[7].

FFT updates (green arrows) follow the conventional spectral evolution and inverse FFT to produce far-field height maps.

WP updates (blue arrows) inject and advect particles inside local patches, and their contributions are accumulated into energy and height maps.

Coupling (orange arrows) blends the WP patches with the FFT background through smooth interpolation, yielding a seamless hybrid ocean.

Object interaction (yellow arrows) lets floating bodies exchange forces with WP patches, generating wakes and ripples while responding to ocean motion.

As FFT updates are standard[21] and interpolation is straightforward, we focus on the design of WP updates and object interaction, which constitute the novel part of our pipeline.

4.2 Discretization and Rendering

The frequency domain is discretized into N_ω buckets of width $\Delta\omega$, so particles in the same bucket share velocity, radius, and kernel, enabling coherent GPU processing. Directions are sampled from the same directional spectrum $S(\omega, \theta)$ as the FFT field, amplitudes use Eq.(7), and the number of particle groups per step N_i follows Eq.(17) to preserve statistical energy consistency.

During synthesis, particles accumulate contributions into layered textures (one per bucket). Each layer is smoothed by two separable passes along x and y , then all layers are summed to form the patch height map. Normals and displacements are derived by finite differences. Finally, patch maps are blended with the

FFT background using smooth distance-based weights, eliminating seams while preserving global continuity and local detail.

4.3 Bidirectional Interaction

To enable two-way coupling, we introduce a spectrum-consistent WP emission mechanism driven by object-water interactions.

On the *object-receives-water* side, buoyancy is computed from the blended height and normal maps at probe points, producing drift under wind waves.

On the *object-acts-on-water* side, displacement and suction effects are estimated from contact volume and relative velocity, and mapped to WP emissions: vertical motions trigger ring ripples, while horizontal components yield Kelvin-like wakes. The total energy of emitted particles equals the displaced water volume. For efficiency, each new particle is assigned to the frequency bucket with the closest radius, avoiding the creation of extra height-map layers and thus reducing rendering cost.

5 Experiments and Results

5.1 Experimental Setup

All experiments were conducted on a desktop workstation. The hardware and software configuration is as table (1).

Table 1. Experimental setup

CPU	13th Gen Intel(R) Core(TM) i7-13700K
GPU	NVIDIA GeForce RTX 4080
Memory	64 GB DDR5@6400 MHz
Engine	Unity 2022.3.26f1

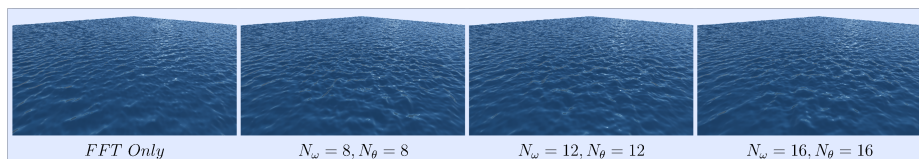
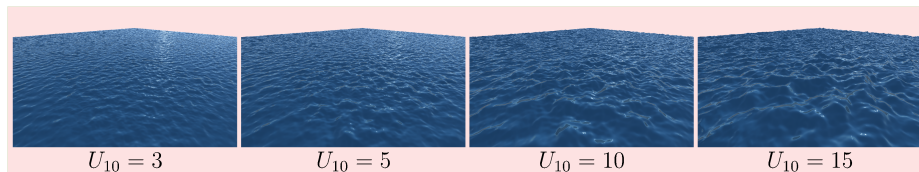
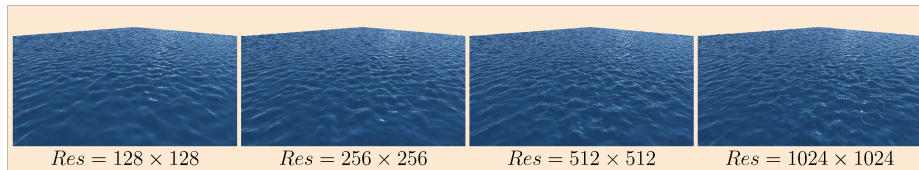
5.2 Results and Performance with Different Parameters

To assess the system’s robustness under parameter variations, we evaluate performance and consistency along three axes: sampling resolution (N_ω, N_θ), wind speed at 10 meters above the sea (U_{10}), and the resolution of the wave particle region (Res). The hybrid ocean results under different parameter settings are shown in Fig.(4), Performance (FPS) is reported in Table.(2). Unless otherwise specified, the default parameter values are:

- $N_\omega = 16, \quad N_\theta = 16$
- $U_{10} = 5, \quad FetchSize = 10000$
- $Res = 512 \times 512$
- $OceanSize_{FFT} = 500 \times 500, \quad OceanSize_{WP} = 100 \times 100$

Table 2. Performance with different parameters

Method	(N_ω, N_θ)	U_{10}	Res	FPS
FFT-Only	\	5	512×512	2000+
WP-Only	(16,16)	5	512×512	4
Hybrid (Ours)	(16,16)	5	512×512	86
Hybrid (Ours)	(12,12)	5	512×512	139
Hybrid (Ours)	(8,8)	5	512×512	306
Hybrid (Ours)	(16,16)	5	256×256	89
Hybrid (Ours)	(16,16)	5	1024×1024	56
Hybrid (Ours)	(16,16)	3	512×512	39
Hybrid (Ours)	(16,16)	10	512×512	220
Hybrid (Ours)	(16,16)	15	512×512	318

(a) Results with different sample counts (N_ω, N_θ) (b) Results with different wind speeds (U_{10}) (c) Results with different WP-Patch resolutions (Res) **Fig. 4.** Results with different parameters

Sample Count (N_ω, N_θ) Increasing N_ω and N_θ refines frequency-direction discretization, producing more particles and richer local detail. Since amplitudes follow Eqs. 7 and 17, energy is redistributed rather than amplified, reducing spectral bias. Particle generation and accumulation cost grows roughly linearly with sampling, but frequency bucketing keeps it manageable; visual improvements saturate beyond (16, 16).

Wind Speed (U_{10}) As U_{10} rises, wave height increases while JONSWAP concentrates energy near ω_p , suppressing high-frequency tails. Fewer short-wave

particles are spawned, lowering per-frame cost; performance therefore improves at higher winds without losing near- or far-field fidelity.

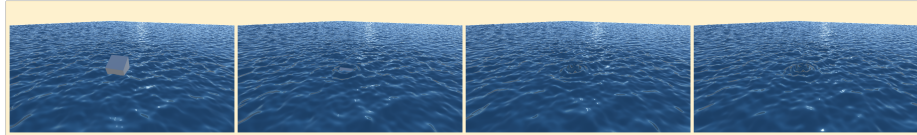
Patch Resolution (Res) Higher Res yields more accurate energy maps but increases filtering cost. Below 512^2 , overhead is negligible; above 1024^2 , cost rises sharply while visual gains remain minor.

Overall, different platforms can choose (N_ω, N_θ) and Res for the desired balance of quality and speed. Across tested settings, WP-FFT surfaces remain spectrally consistent, and the propagation speed of dominant long waves matches between WP and FFT solutions, even if this is difficult to show in still figures.

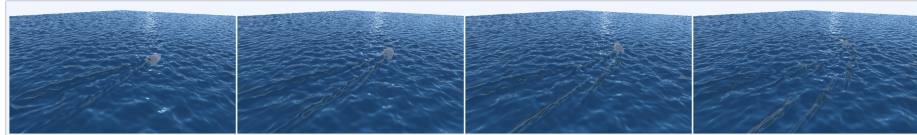
5.3 Interactions between Different Objects and Ocean

As illustrated in Fig. 5, our system supports realistic bidirectional interactions between rigid props, boats, and the hybrid ocean surface. Objects respond to ocean forces through buoyancy drift, while at the same time generating ripples and wakes consistent with their volume and velocity.

This demonstrates a key advantage of our hybrid model: unlike FFT-only oceans, which cannot represent wakes/ripples, or WP-only methods whose large-scale simulation is constrained by performance limitations, our method enables localized, spectrum-consistent interactions embedded in a large-scale ocean.



(a) Interactions between Simple Cube and Ocean



(b) Interactions between Boat and Ocean

Fig. 5. Interactions between Different Objects and Ocean

6 Conclusions and Future Work

6.1 Conclusions

We presented a real-time hybrid ocean framework that couples a global FFT background with local wave-particle (WP) patches under a unified spectrum. The

framework introduces two key innovations: (i) a spectrum-consistent WP-FFT representation that seamlessly integrates large-scale spectral stability with localized interactions, and (ii) an efficient frequency-bucketed sampling and GPU-parallel synthesis scheme that maintains spectral consistency while sustaining real-time performance.

Extensive experiments under varying spectral and sampling parameters validate the effectiveness of our approach: the system consistently reproduces coherent wakes and ripples while preserving near-far continuity and interactive performance. These results demonstrate that the proposed method bridges the gap between large-scale spectral realism and fine-grained interactivity in real time.

6.2 Limitations and Future Work

Although effective, our framework has two main limitations. First, information exchange between the FFT background and WP patches is incomplete: ripples generated in WP regions do not propagate back to the far-field FFT surface, and new particles are not sampled from the instantaneous FFT boundary state, which can reduce cross-boundary coherence. Second, the system lacks adaptive sampling: parameters such as (N_ω, N_θ) and patch resolution remain fixed, rather than adjusting to hardware capability or environmental conditions (e.g., wind speed), leading to uneven performance across scenarios.

Future work will focus on addressing these issues, by designing a truly bidirectional boundary coupling mechanism that exchanges energy and phase information between FFT and WP, and developing adaptive sampling strategies that dynamically balance visual fidelity and frame rate across different devices and environments.

Acknowledgments. We thank the members of the DALab at Shanghai Jiao Tong University for their insightful discussions and continuous support throughout this work.

Disclosure of Interests. The authors declare no conflicts of interest.

References

1. Agrotis, A.: „a fluid implicit particle (flip) solver built in houdini,“. Bournemouth University, NCCA (2016)
2. Bowles, H., Zimmermann, D., Noris, G., Wang, B.: Crest: Novel ocean rendering techniques in an open source framework. In: Siggraph 2017 Advances in Real-Time Rendering in Games (2017)
3. Donatini, L., Verwilligen, J., Delefortrie, G., Vantorre, M., Lataire, E.: Physically accurate real-time synthesis of ocean waves for maritime simulators. *Applied Ocean Research* **143**, 103866 (2024)
4. Flügge, F.J.: Realtime gpgpu fft ocean water simulation (2017)

5. Forristall, G., Ewans, K.: Worldwide measurements of directional wave spreading. *Journal of Atmospheric and Oceanic Technology - J ATMOS OCEAN TECHNOL* **15** (04 1998). [https://doi.org/10.1175/1520-0426\(1998\)015<0440:WMODWS>2.0.CO;2](https://doi.org/10.1175/1520-0426(1998)015<0440:WMODWS>2.0.CO;2)
6. Fournier, A., Reeves, W.T.: A simple model of ocean waves. In: *Proceedings of the 13th annual conference on Computer graphics and interactive techniques*. pp. 75–84 (1986)
7. Fréchet, J.: Realistic simulation of ocean surface using wave spectra. In: *Proceedings of the first international conference on computer graphics theory and applications (GRAPP 2006)*. pp. 76–83 (2006)
8. Horvath, C.J.: Empirical directional wave spectra for computer graphics. In: *Proceedings of the 2015 Symposium on Digital Production*. pp. 29–39 (2015)
9. Huang, L., Qu, Z., Tan, X., Zhang, X., Michels, D.L., Jiang, C.: Ships, splashes, and waves on a vast ocean. *ACM Transactions on Graphics (TOG)* **40**(6), 1–15 (2021)
10. Jeschke, S., Skřivan, T., Müller-Fischer, M., Chentanez, N., Macklin, M., Wojtan, C.: Water surface wavelets. *ACM Transactions on Graphics (TOG)* **37**(4), 1–13 (2018)
11. Jeschke, S., Wojtan, C.: Water wave packets. *ACM Transactions on Graphics (TOG)* **36**(4), 1–12 (2017)
12. Kythe, P.K.: *An introduction to boundary element methods*. CRC press (2020)
13. Macklin, M., Müller, M.: Position based fluids. *ACM Transactions on Graphics (TOG)* **32**(4), 1–12 (2013)
14. Mastin, G.A., Watterberg, P.A., Mareda, J.F.: Fourier synthesis of ocean scenes. *IEEE Computer graphics and Applications* **7**(3), 16–23 (2007)
15. Mazzaretto, O.M., Menéndez, M., Lobeto, H.: A global evaluation of the jonswap spectra suitability on coastal areas. *Ocean Engineering* **266**, 112756 (2022)
16. Mitsuyasu, H., Tasai, F., Suhara, T., Mizuno, S., Ohkusu, M., Honda, T., Rikiishi, K.: Observations of the directional spectrum of ocean waves using a cloverleaf buoy. *Journal of Physical Oceanography* **5**(4), 750–760 (1975)
17. Müller, M., Charypar, D., Gross, M.: Particle-based fluid simulation for interactive applications. In: *Proceedings of the 2003 ACM SIGGRAPH/Eurographics symposium on Computer animation*. pp. 154–159 (2003)
18. Newell, A.C., Zakharov, V.E.: The role of the generalized phillips' spectrum in wave turbulence. *Physics Letters A* **372**(23), 4230–4233 (2008)
19. Pan, F., Zou, L., Dong, D., Xiao, S.: Simulation of ocean waves with spectrum-based wave particle. *Computer Animation and Virtual Worlds* **36**(2), e70014 (2025)
20. Stewart, R.H.: *Introduction to physical oceanography* (2008)
21. Tessenor, J., et al.: Simulating ocean water. *Simulating nature: realistic and interactive techniques. SIGGRAPH* **1**(2), 5 (2001)
22. Tian, Z., Perlin, M., Choi, W.: Frequency spectra evolution of two-dimensional focusing wave groups in finite depth water. *Journal of Fluid Mechanics* **688**, 169–194 (2011). <https://doi.org/10.1017/jfm.2011.371>
23. Yuksel, C., House, D.H., Keyser, J.: Wave particles. *ACM Transactions on Graphics (TOG)* **26**(3), 99–es (2007)